IJBPAS, May, 2017, 6(5): 953-975

ISSN: 2277–4998

International Journal of Biology, Pharmacy and Allied Sciences (IJBPAS)

'A Bridge Between Laboratory and Reader'

www.ijbpas.com

NANOTECHNOLOGY BASED APPROACH TO ENHANCE THE POTENTIAL OF CHEMOPREVENTIVE AGENT BERBERINE HYDROCHLORIDE IN CANCER THERAPY

MD ALI MUJTABA[1*], KHIDIR A. M. HASSAN[1]

[1]Department of Pharmaceutics, Faculty of Pharmacy, Northern Border University, Rafha, Kingdom of Saudi Arabia

***Corresponding Author: Dr. Md. Ali Mujtaba, Assistant Professor, Department of Pharmaceutics, Faculty of Pharmacy, Northern Border University, Rafha Kingdom of Saudi Arabia; E- mail: sajanqa@gmail.com, mohammed.Mujtaba@nbu.edu.sa**

Mobile: +919891611864, +966538156614

Received 23rd March 2017; Revised 29th March 2017; Accepted 13th April 2017; Available online 1st May

ABSTRACT

Berberine hydrochloride (BHC) is an isoquinoline alkaloid that possesses promising antitumor activities. Nevertheless, the therapeutic agent of this substance in cancer is limited because of low aqueous solubility which limits its bioavailability and hence therapeutic effects. Therefore, the aim of the present study was to develop a chitosan (CH)-sodium alginate (SA) nanoparticles of BHC with a view to improve its aqueous solubility. It was optimised using design of experiments by employing a 3-factor, 3-level Box-Behnken statistical design. Independent variables studied were the amount of the polymers: CH, SA and the amount of BHC in the formulation. The dependent variables were the particle size, zetapotential and encapsulation efficiency. Response surface plots were drawn, statistical validity of the polynomials was established and optimised formulations were selected by feasibility and grid search. Nanoparticles were characterised by FT-IR, DSC and TEM. Drug loading, encapsulation efficiency and particle size, size distribution (polydispersity index) and zetapotential were determined. The optimized nanoparticles have average particle size from 251nm (polydispersity 0.347) and zetapotential 25.73 mV. Nanoparticles revealed a fast release during the first 2 hour followed by a continuous and controlled drug release during a 24-h period following a non-Fickian diffusion process. Our studies demonstrated that the new

CH-SA NPs system of BHC is a promising strategy for improving solubility and in turn, therapeutic efficacy of BHC. The overall results suggest that CH-SA NPs could be a potential option for BHC delivery.

Keywords: Nanoparticles; chitosan; alginate; berberine; Box-Behnken design

1. INTRODUCTION

Natural compounds are emerging as effective agents for the treatment of malignant diseases. Berberine is a natural isoquinoline alkaloid isolated from medicinal herbs such as Coptis chinensis and Hydrastis canadensis, and has diverse pharmacological actions. Nowadays, anti-inflammatory and antitumor activities of berberine have made it a vital chemotherapeutic agent for cancer chemotherapy [1]. Berberine has an inherent property of cell cycle arrest and induction of apoptosis in tumor cells followed by impairment of cellular dynamics and invasion by regulation of an array of molecular circuits [2-4]. Potent antitumor activity of berberine is also due to its multi-pronged actions such as generation of reactive oxygen radicals, inhibition of DNA gyrase activity and NFκB signal activation of p53 genes [5-7]. Regardless considerable promise that berberine is an efficacious and safe compound for cancer therapy and chemoprevention. However, due to its hydrophobic nature, poor stability and low bioavailability, the actual therapeutic application of berberine is hampered for a long time. Poor water solubility of berberine reflects in limited absorption in the gastrointestinal tract and subtherapeutic plasma concentrations. These issues have hindered the development of berberine as a pharmaceutical formulation. So a novel delivery system to improve the solubility and bioavailability of BR is a matter of exigency.

Nanoparticle is a platform for delivery system that is widely used in biological field for its increased pharmacodynamic action, improved bioavailability and targeting effect, especially in anti-tumor activity [8]. Modern nanoparticulate dosage forms including polymeric nanoparticles, nanocapsules, liposomes, solid lipid nanoparticles, and nanoemulsions, all of which can improve drug solubility. Nanoparticles consisting of synthetic biodegradable polymers, natural biopolymers, lipids and polysaccharides have been developed and tested over the past decades. Recently, the idea of using nanoparticles made from natural biodegradable polymers to deliver drugs has provoked great interests. The interaction between biodegradable cationic and anionic biopolymers leads to the formation of polyionic hydrogels, which have demonstrated favourable characteristics for drug entrapment and delivery. Chitosan (CH) and Sodium alginate (SA) are two biopolymers that have received much attention and have been extensively studied for such use [9]. CH is a natural polysaccharide polymerized by β (1–4) linked D-glucosamine residues; this polysaccharide has been extensively researched as a delivery system for its non-toxicity, biocompatibility and biodegradability, polycationic properties, and the presence of amino groups along the CH chain [10]. CH being a cationic polymer has been used for the production of microspheres and nanoparticles by ionotropic gelation with negatively charged polymers and there are many chitosan–polyanion complexes that have been investigated as drug delivery systems for drugs, proteins, DNA and other oligonucleotides, with encouraging results [11–13]. Among the various types of chitosan–polyanion complexes reported in the literature, the combination of CH and SA is considered to be the most interesting for colloidal carrier systems [14]. The advantage of this delivery system is its non-toxicity permitting the repeated administration of therapeutic agents.

Thus the objective of the present study was to evaluate the possibility of CS-SA nanoparticles as carriers for berberine. The challenge was to entrap a hydrophobic molecule into hydrophilic nanoparticles formed by ionotropic gelation of the positively charged polysaccharide chitosan and polyanion alginate. Hence, the current study aimed at developing and optimising nanoparticulate formulation of berberine using design of experiments by employing Box-Behnken statistical design (BBD). The BBD-based optimization was employed to evaluate the effect of three independent process variables i.e., concentration of sodium alginate (X_1), chitosan (X_2) and BBR (X_3) on the properties of nanoparticles, like particle size (nm), Zetapotential and drug encapsulation efficiency (DEE). Another aim was to undertake a physicochemical characterization of the optimal formulation in terms of release kinetics, thermal properties, infrared spectroscopy, surface morphology and stability studies.

2. Materials and Methods

2.1. Materials

Chitosan with medium molecular weight and degree of deacetylation about 85% were purchased from Sigma–Aldrich, St. Louis, MO, USA. The medium viscosity sodium alginate isolated from Macrocystis pyrifera, having molecular weight between

75 and 100 kDa, and mannuronic to guluronic acid ratio of 1.5 (60:40), was purchased from CDH Labs., India. Berberine hydrochloride (BHC) and all other reagents and chemicals used were of analytical reagent grade.

2.2. Preparation of BHC loaded CH-SA nanoparticles (NPs)

BHC loaded CH-SA NPs were prepared using modified method. Both the SA and CH solutions were prepared by dissolving the polymers in distilled water. The pH of the SA solutions was (5.0–5.3) adjusted using hydrochloric acid. The CH was dissolved in 1% acetic acid solution and pH was adjusted to 5 ± 0.1 using 0.1 N NaOH solutions. The SA and CH solutions were filtered under vacuum before use in NPs preparation. The drug BHC was stirred with SA solution to form the drug-alginate complex. The CH solution was stirred with polaxamer 188 (0.50% w/v) at 60°C for 2 h to obtain a homogeneous mixture and this solution was gradually dropped to the alginate-BBR complex over 1 h while stirring at 1000 rpm. The stirring was continued for another half an hour and then equilibrated overnight to allow nanoparticles to form uniform particle size. polaxamer 188 (0.50% w/v) was added to aid in solubilisation of BHC. Nanoparticles were formed as a result of the interaction between the negative groups of SA and the positively charged amino groups of CH (ionotropic gelation). Nanoparticles were collected by centrifugation at 18,000 rpm for 30 min at 4^{o}C.

Different CH–SA NPs formulations of BHC were prepared using the following composition: SA (0.2–0.6% w/v), CH (0.1–0.2% w/v) and BHC (0.01–0.10% w/v). Various formulations were prepared using the Box-Behnken experimental design (BBD). The range of the two polymers under study was selected on the basis of preliminary experimentation where three kinds of phenomenon were observed: almost clear solutions, opalescent suspensions and aggregates. The zone of opalescent suspensions was of our interest for preparing nanoparticulate systems and it was further examined and optimised using design of experiments i.e. BBD.

2.3 Experimental design

Systematic optimization procedures are carried out by selecting an objective function, finding the most important or contributing factors and investigating the relationship between responses and factors by the so-called response surface methodology (RSM) [15]. To understand the variables and their interactions, many statistical experimental designs have been recognized as useful techniques. RSM is one of the popular methods in the development and optimization of drug delivery systems. Based on the principles of design of experiments (DOE), the methodology involves the use of various types of experimental designs, generation of polynomial mathematical relationships and mapping of the response over the experimental domain to select the optimum formulation [16]. The BBD is one of the most efficient DOE methods. The advantage of this design is that it does not contain combinations for which all factors are simultaneously at their highest or lowest levels. So these designs are useful in avoiding experiments performed under extreme conditions, for which unsatisfactory results are often obtained. Additionally, it requires fewer experimental runs and less time and thus provides a far more effective and cost-effective technique than the conventional processes of formulating and optimization of dosage forms. So BBD was used to statistically optimise the formulation parameters and evaluate the main effects, interaction effects and quadratic effects of the formulation ingredients on the particle size (Y_1), Zetapotential (Y_2) and % encapsulation efficiency (Y_3). A three-factor, three-level design was used because it was suitable for exploring quadratic response surfaces and constructing second order polynomial models for optimization using Design Expert® (Version 8.0.7.1, Stat-Ease Inc., Minneapolis, Minnesota). The non-linear quadratic model generated by the design is given as:

$$\mathbf{Y_o = b_o + b_1X_1 + b_2X_2 + b_3X_3 + b_{12}X_1X_2 + b_{13}X_1X_3 + b_{23}X_2X_3 + b_{11}X^2_1 + b_{22}X^2_2 + b_{33}X^2_3} \quad \textbf{(1)}$$

Where Y_o is the dependent variable; b_0 is an intercept; b_1 to b_{33} are regression coefficients computed from the observed experimental values of Y; and X_1, X_2 and X_3 are the coded levels of independent variables. The terms $X_{1,}$ X_2 and X_i (i = 1, 2 or 3) represent the interaction and quadratic terms, respectively [17]. This experimental design was used to investigate the effect of independent variables on various dependent variables. The independent variables were % w/v of SA concentration (X_1), % w/v of CH concentration (X_2) and % w/v of BHC concentration (X_3) represented by -1, 0, +1, analogous to the low, middle and high levels respectively, while the dependent variables were particle size (Y_1), Zetapotential (Y_2) and % encapsulation efficiency (Y_3) as described in Table 1. The concentration of SA (X_1), CH (X_2) and BHC (X_3) used to prepare the 17 experimental formulations and the corresponding observations for dependent variables are given in Table 2.

2.4 Physiochemical Characterisation of nanoparticles

2.4.1. Particle size and zetapotential measurements

The average particle size and size polydispersity of the nanoparticles dispersed in distilled water were determined by dynamic light scattering technique at 25 °C using a particle size analyzer (Zetasizer Nano ZS, Malvern Instruments, UK). The zeta potential of nanoparticles was measured using the Zeta potential analyzer (Zetasizer Nano ZS, Malvern Instruments, UK). All measurements were performed in triplicate. The zeta potential is considered as one of the highest measured parameters which denotes the overall charges acquired by the particles in a particular medium and it is considered as one of the important factors for the stability of the nanoparticles.

2.4.2. Determination of entrapment efficiency and drug loading

The entrapment efficiency (EE) and drug loading (DL) capacity of the nanoparticles formulation was determined by the separation of drug-loaded nanoparticles from the aqueous medium containing non-associated BBR by ultracentrifugation (REMI high speed, cooling centrifuge, REMI Corporation, India) at 18,000 rpm for 30 min. The amount of BHC loaded into the nanoparticles was calculated as the difference between the total amount used to prepare the nanoparticles and the amount that was found in the supernatant. The amount of free BHC in the supernatant was measured by spectrophotometrically (λ_{max} 343 nm; Shimadzu Model 1601, Tokyo, Japan). The EE and DL was determined by the following equations:

$$\textbf{EE (\% w/w)} = \frac{W1-W2}{W1} \times 100$$

$$\textbf{Drug loading (\%w/v)} = \frac{W1-W2}{W3} \times 100$$

Where W_1 = amount of drug added in the nanoparticle, W_2 = amount of un-entrapped drug and W_3 = weight of nanoparticles

2.4.3. Transmission electron microscopy (TEM) analysis

The formulation was observed under TEM to determine the surface morphology and size of the formulation. The nanoparticles sample was diluted using aqueous phase and stained negatively by phosphotungstic acid and finally dried on carbon coated grid. This was observed using TEM (JOEL, 2100F, USA) which operates at 200kV.

2.4.4. Fourier transform infra-red spectroscopy (FT-IR)

CS–SA NPs separated from nanoparticulate suspensions were dried by a freeze dryer, and their FT-IR transmission spectra were obtained using a FT-IR-8300 spectrophotometer (Shimadzu, Japan). A total of 2% (w/w) of sample, with respect to the potassium bromide disc, was mixed with dry KBr. The mixture was ground into fine powder using an agate mortar before compressing into KBr disc under a hydraulic press at 10,000 psi. Each KBr disc was scanned at 4 mm/s at a resolution of 2 cm over a wave number region of 400–

4000 cm^{-1} using IR software (ver. 1.10). The characteristic peaks were recorded for different samples.

2.4.5. Differential scanning calorimetry

Differential scanning calorimetric (DSC) analysis was used to characterise the thermal behaviour of the individual polymers, BHC and BHC loaded NPs. DSC thermograms were obtained using an automatic thermal analyzer system (Pyris 6 DSC, Perkin-Elmer, USA). Temperature calibration was performed using Indium calibration reference standard as a standard. Samples were crimped in standard aluminum pans and heated from 40 to 400 ^{o}C at a heating rate of 10 ^{o}C/min under constant purging of dry nitrogen at 20 ml/min. An empty pan, sealed in the same way as the sample, was used as a reference.

2.4.6. In vitro **release kinetics studies**

The *in vitro* dissolution studies were carried out to compare the release of drug form the optimized nanoparticulate formulation to observe the release pattern. The *in vitro* release study of the plain BHC solution and BHC loaded CH-SA NPs formulation was performed using dialysis bag technique in the phosphate buffer solution (PBS) pH 6.8 [18]. The dialysis bag (M.W 12 kDa, Sigma–Aldrich) was activated as per the procedure and was soaked in the dissolution medium for 24 h. Nanoparticles equivalent to 10 mg of drug was placed in a cellulose dialysis bag, (MWCO 12,000 g/mole; Sigma, St. Louis, USA) and to this a little amount of dissolution media was added, which was then sealed at both ends. The dialysis bag was dipped into the receptor compartment containing the dissolution medium, which was stirred continuously at 50 rpm maintained at 37 °C. The samples (5 ml) were withdrawn at predetermined time intervals, filtered through syringe filter (0.45 μm, Millipore, Mumbai, India) and analyzed immediately after the completion of dissolution test by UV–vis spectrophotometer. Equal volume of pH 6.8 phosphate buffer was replaced into the vessel after each sampling. BHC dissolved in the dissolution media was measured at λ_{max} 343 nm and the plot between cumulative amounts of drug release vs. time was plotted.

Data obtained from *in vitro* release studies were fitted to various kinetic equations to find out the mechanism of drug release from CH-SA NPs. Kinetic analysis of drug release of BHC from CH-SA NPs was performed using various mathematical models such as zero order, first order, Higuchi, Hixon-Crowell and Korsemeyer-Peppas models [19–21].

2.4.7. Optimisation data analysis and model-validation

ANOVA provision available in the software was used to establish the statistical validation of the polynomial equations generated by Design Expert®. Suitable models for mixture designs consisting of three components include linear, quadratic and special cubic models. The best fitting mathematical model was selected based on the comparisons of several statistical parameters including the coefficient of variation (CV), the multiple correlation coefficient (R^2), adjusted multiple correlation coefficient (adjusted R^2; and the predicted residual sum of square (PRESS), proved by Design-Expert® software. Among them, PRESS indicates how well the model fits the data, and for the chosen model it should be small relative to the other models under consideration [22]. Three dimensional response surface plots were provided by the Design Expert® software, where by intensive grid search performed over the whole experimental region, the optimum checkpoint formulations were selected to validate the chosen experimental domain and polynomial equations. The optimized checkpoint formulations were prepared and evaluated for various response properties. The resultant experimental values of the responses were quantitatively compared with that of the predicted values to calculate the percentage prediction error.

2.4.10. Stability studies

The lyophilized CH-SA nanoparticles were subjected to stability studies for 90 days in a desiccator at room temperature. Lyophilized nanoparticles were reconstituted with milli-Q water under gentle agitation. Reconstituted sample was analyzed for particle size, entrapment efficiency and Zeta potential on 0, 30 and 90 days.

3. RESULTS AND DISCUSSION

3.1. Preparation of CH-SA NPs

The preparation of CS–SA NPs, based on an ionotropic gelation process, involves mixing the two aqueous phases at room temperature. The ionotropic gelation process did not include emulsification step and stage of organic solvents, thereby minimizing inactivation of encapsulated drugs. The preparation of BHC loaded CH-SA NPs are relatively difficult. Because BHC is hydrophobic, these hydrophilic nanoparticles are used to encapsulate hydrophobic drug is not clear. A number of experiments had to be performed in order to determine the appropriate conditions for the incorporation of the hydrophobic BHC into the CH-ALG nanoparticles. Because of the higher viscosity of CH solution, a number of experiments were performed by varying the concentration of CH and SA, in order to screen the appropriate concentration range so as to allow the formation of turbid solutions and not the aggregates. The final concentration range selected for optimisation study was 0.2–0.6% w/v SA and 0.1–0.2% w/v for CH respectively. The drug concentration range selected was from 1:1 to 1:10 with respect to CH. Initially, the CH droplet formation occurred with the stirring with polaxamer 188, followed by the droplet solidification by ionically crosslinking of the alginate solution. In aqueous solutions with pH around 5.2 the amine groups of the CH are protonated and the carboxyl groups of the SA are ionised, which is most important for optimum interaction and the polyionic complex formation [23]. Also pH 5.2 amino groups of interacted with alginate carboxylate groups to form the hydrogel. Since alginate is a negatively charged polymer the positively charged BHC was complexed initially with alginate to obtain a higher loading of the drug to the nanoparticle.

3.2. Experimental design

For the response surface methodology involving BBD, a total of 17 experiments (BB1–BB17) were performed for three factors at three levels each. This number is equal to the midpoint of each edge and the three replicated centerpoints of the cube. The experiment runs with independent variables and the observed responses for the 17 formulations are shown in Table 2.

3.3. Fitting data to model

All the responses observed for 17 formulations prepared were simultaneously fitted to different models using Design-Expert®. The fit summary for each response was shown in Table 3. In order to evaluate the effect of independent variables on the each of dependant responses Y_1–Y_3, the causal factor and response variables were related using polynomial equation with statistical analysis. The comparative values of multiple correlation coefficient (R^2), adjusted multiple correlation coefficient (adjusted R^2), S.D., %C.V. and the predicted residual sum of squares (PRESS) are presented in Table 3. Responses Y_1, Y_2 and Y_3 were found to follow quadratic model, because its PRESS was smallest. Only statistically significant ($p < 0.05$) coefficients are included in the equations. Predicted residual sum of squares (PRESS) is a measure of the fit of the model to the points in the design. The smaller the PRESS statistic is, the better the model fits to the data points [24]. The model showed a statistically insignificant lack of fit. The adequacy of the model was also confirmed with residual plot tests of regression models. Analysis of variance (ANOVA) was applied to estimate the significance of the model at the 5% significance level.

3.4. Contour plots and response surface analysis by polynomial Equation

Two-dimensional contour plots and three dimensional response surface plots, as presented in Figure 1, are very useful to see interaction effects of the factors on the responses. These types of plots show effects of two factors on the response at a time. In all the presented figures, the third factor was kept at level zero.

3.4.1. Response 1 (Y_1): effect on particle size

The following polynomial equation was generated for particle size of nanoparticles.

$$Y_1 = 306.80 + 26.69\,X_1 + 8.16\,X_2 + 5.37\,X_3 - 3.33\,X_1X_2 + 13.25\,X_1X_3 - 3.00\,X_2X_3 - 8.99\,X_1^2 + 49.76\,X_2^2 + 10.44\,X_3^2$$

Where Y_1 is Particle size of the developed NPs and X_1, X_2, X_3 are the concentration of SA, CH, and Drug respectively. The model F-value of 110.30 implies that the model is significant. The "Pred R-Squared" of 0.8942 is in reasonable agreement with the "Adj R-Squared" of 0.9840; i.e. the difference is less than 0.2. "Adeq Precision" measures the signal to noise ratio. A ratio greater than 4 is desirable. My ratio of 33.196 indicates an adequate signal. This model can be used to navigate the design space.

There is a direct relationship between the particle size and the polymer concentrations and at a constant concentration of 0.10% w/v of CH, the particle size of the nanoparticles was found to vary between 216.5 nm and 278.4 nm depending upon the SA concentration. At 0.20% w/v concentration of CS the nanoparticles size varied between 423.4 nm and >450 nm, respectively, depending upon the concentration of SA (Table 2). It can be observed that the nanoparticles size, is dependent upon the concentration of two polymers (CH and SA), the minimum size i.e. 216.5 nm, corresponding to the lowest CH and SA concentration and the maximum size i.e. 488 nm, corresponding to the highest CH and SA concentrations. These results confirm that smaller nanoparticles result, when the availability of the functional groups on two polymers for interaction is in stoichiometric proportion [25].

3.4.2. Response 2 (Y_2): effect on Zetapotential

The model proposes the following polynomial equation for zetapotential:

$$Y_2 = 25.80 - 3.20\,X_1 + 8.16\,X_2 - 0.84\,X_3 - 0.38\,X_1X_2 + 0.17\,X_1X_3 + 0.58\,X_1^2 + 5.75\,X_2^2 - 8.75\,X_3^2$$

The model F-value of 48.08 implies the model is significant. The "Pred R-Squared" of 0.7763 is in reasonable agreement with the "Adj R-Squared" of 0.9636; i.e. the difference is less than 0.2. "Adeq Precision" measures the signal to noise ratio. A ratio greater than 4 is desirable. The ratio of 25.046 indicates an adequate signal. This model can be used to navigate the design space. The zetapotential of the NPs was primarily affected by the CH concentration and can be ascribed to the higher availability of protonated amine groups with increasing CH concentration. Zetapotential of the CH–SA NPs systems was dependent upon the availability of total protonated $–NH_2$ group on CH and its neutralisation with $–COO^-$ groups of SA. Higher the availability of $–NH_2$ groups (at higher CH concentration) and lower the neutralisation of these with $–COO^-$ groups (at lower concentration of ALG), higher was the zetapotential.

3.4.3. Response 3 (Y_3): effect on Encapsulation efficiency

The following polynomial equation was proposed by the model for Encapsulation efficiency (EE):

Y_3 = 81.39 -1.86 X_1 - 2.62 X_2 +1.03 X_3 + 0.51 X_1X_2 + 0.082 X_1X_3 + 2.36 X_2X_3 - 2.53 X_1^2 -13.05 X_2^2 - 3.04 X_3^2

The model F-value of 16.52 implies the model is significant. The "Pred R-Squared" of 0.8196 is in reasonable agreement with the "Adj R-Squared" of 0.8972; i.e. the difference is less than 0.2. "Adeq Precision" measures the signal to noise ratio. A ratio greater than 4 is desirable. Your ratio of 11.459 indicates an adequate signal. This model can be used to navigate the design space.

As shown in Table 2, EE of the NPs was found to vary between 60.58% and 85.69%. It was also observed that the encapsulation of BHC into CH–SA nanoparticles was highest (77.76–85.69%) when the CH, SA and the drug were used at intermediate concentrations, whereas the encapsulation was found to be less than 70% when either of the CH or SA is used at higher concentration levels. It can be explained on the basis of the fact that at higher concentrations of the two polymers, which make the bulk of the nanoparticles matrix and less volume is available for drug encapsulation.

3.5. Optimization and validation of RSM results

Point prediction of the design expert software was used to determine the optimized composition which predicted the optimized process parameters to be 255.43nm for particle size, 26.43mV for zetapotential and 81.21% for drug encapsulation efficiency of nanoparticle formulation at SA concentration 0.26%w/v, CH 0.14%w/v and BHC 0.054%w/v. The optimized nanoparticle formulation was prepared. The composition of optimum check point formulations, their predicted and experimental values for all the response variables and the percentage error in prognosis are shown in Table 4. For all the checkpoint formulation, the results of the evaluation for particle size, zetapotential and encapsulation efficiency were found to be within limits. The percentage prediction error assures the validity of generated equations and thus depicts the domain of applicability of RSM model. Linear correlation plots between the actual and the predicted response variables were plotted Figures 2a–2c and the residual plots showing the scatter of the residuals versus actual values are presented in Figures 2d–2f. Linear correlation plots between the actual and the predicted response variables showed the scatter of the residuals versus actual values to better represent the spread of the dependent variables under present experimental settings. Thus the low magnitudes of errors as well as the significant values of R^2 in the present investigation prove the high prognostic ability of the Box-Behnken designs.

3.6. Physiochemical characterization of the optimized formulation

The optimal formulation identified via the Box–Behnken design was characterized in terms of Particle size, zeta potential, entrapment efficiency, drug loading. *In vitro* release studies, drug release mechanisms, thermal behaviour, FTIR analysis and morphology and the results are presented hereunder.

3.6.1. Particle size and zeta potential measurements

The particle size and PDI of the optimized CH-SA nanoparticles were 251.29 ± 1.85 nm and 0.347 ± 0.087 (n = 3) respectively as shown in the Figure 3(a). The zeta potential was found to be 25.73 ± 0.865 mV (n = 3) shown in the Figure 3(b). Dynamic light scattering technique measures the fluctuation of the intensity of the scattered light due to the particle movement in the diluted sample of the nanoparticle. A low PDI value is considered as optimal as it indicates a higher homogeneity of the particle in the formulation. The zeta potentials of BHC loaded CH-SA NPs show large positive values reflecting the stability of the colloidal suspensions (Table 2). Having positively charged surfaces is an added advantage when using NPs in drug delivery since they are able to transfer easily through negative channels in the cell membrane. An increased zeta potential value with BHC loaded CH-SA NPs was caused by the higher amount of positively charged BHC encapsulation with CH-SA NPs. The out-layer of CH can not only favour nanoparticles positive surface charge, but also prolong the time that the active ingredients contact with the intestinal epithelia and enhance absorption via the para-cellular transport pathway through the tight junctions at neutral and alkaline pH environments [26].

3.6.2. *Determination of entrapment efficiency, drug loading and TEM analysis:*

The % EE of CH-SA NPs was 80.91% ± 1.23 and % DL was 61.68% ± 0.867 (n = 3) respectively. The %EE acts as an important factor influencing the drug release, as well as the overall efficacy of the production process. The CH-SA NPs protects the encapsulant, has biocompatible and biodegradable characteristics, and limits the release of encapsulated materials more effectively than either alginate or chitosan alone [25, 27].

TEM analysis confirmed the presence of nanoparticles and provided morphological information of the BHC loaded CH-SA nanoparticles. With TEM, the NPs were seen to be distinct, spherical particles with solid dense structure (Figure 4). However, the NPs did not show a smooth surface but a fluffy appearance. NPs appeared to be considerably smaller when viewed with TEM as compared to the average particle size observed with DLS. The sizes obtained from DLS technique were larger than the sizes obtained from TEM since DLS measures the hydrodynamic diameter. Also the larger particle size might be due to the swellability of polymeric hydrogels in the solution [25].

3.6.3. Identification of nanoparticles constituents

CH, SA and CS–SA nanoparticles were analysed using FT-IR spectrophotometer for characteristic absorption bands, indicative of their interaction. In order to examine the interaction between the components of nanoparticulate systems, preliminary concerns were taken over polymers interactions. It is well established that the carboxyl group of the SA polymer may interact with the amino group of Chitosan, and form an ionic complex (15). The characteristic peak observed at 1447 cm^{-1} (salt of carboxyl group) in the FT-IR spectrum of NPs was attributed to the ionic interaction between these two reactive groups. Observed changes in the absorption bands of the amino groups, carboxyl groups, and amide bonds could be attributed to an ionic interaction between the carbonyl group of alginate and the amide group of chitosan [28]. DSC thermograms of the CH, SA and BHC showed characteristic endothermic peaks at 92.2 ^{o}C, 103.5 ^{o}C and 191.6 ^{o}C respectively. The characteristic peak for BHC was found to be reduced in intensity and shifted, probably because of encapsulation in CH–SA nanoparticles.

3.6.4. In vitro dissolution study

Figure 5a shows the cumulative release curves of BHC from CH-SA NPs and BHC powder drug at pH 6.8 at 37 ±0.5°C as a function of time. BHC release from CH-SA NPs was significantly rapid as well as complete than the BHC powder. The release profile of CH-SA NPs was characterized by an initial burst effect in the media at first two hour, followed by a continuous and controlled release phase within 24 hour. As shown in Figure 5a within the first two hour, 75.34% drug release is evident in the release curve at pH6.8. The initial fast release of BHC may be due to the rapid hydration of nanoparticles due to the hydrophilic nature of CH and SA. The release medium penetrates into the particles and dissolves the entrapped BHC and, therefore, it could be proposed that the major factor determining the drug release from NPs is its solubilisation or dissolution rate in the release medium.

3.6.5. Release Kinetics

The drug release data were plotted in various kinetic models including zero-order, first order, Higuchi, Korsmeyer-Peppas and Hixson Crowell equation (Figures 5b-5f). From the analysis of Table 5 it was found that the *in vitro* drug release of NPs was best explained by first order, as the plots showed the highest linearity (R^2= 0.9893). However, drug release was also found to be close to Higuchi's model (R^2= 0.9393).The release mechanism of CH-SA NPs was best fit-ted to Korsmeyer-Peppas model which indicated a good linearity, R^2= 0.9531. The value of exponent constant (n) was 0.47, which suggesting non-Fickian diffusion process. This is further supported by the fact that the sequential process of polymer hydration, solvent penetration, drug dissolution and/or polymer erosion determine the drug release from hydrophilic matrices [29].

3.7. Stability studies

Lyohipilized BHC loaded CH-SA nanoparticles were evaluated for stability studies at room temperature. Average particle size, zeta potential and entrapment efficiency were evaluated after reconstitution of the nanoparticle at 0, 30 and, 90 days after lyophilization. Results as shown in the Table 6 proved the stability of the nanoparticles at room temperature with no significant ($p < 0.05$) difference in the observations.

Table 1: Independent variables: factors and their levels for the Box-Behnken design

Independent variables	Levels		
	Low (-1)	Medium (0)	High (+1)
X_1 = Sodium Alginate (% w/v)	0.2	0.4	0.6
X_2 = Chitosan (% w/v)	0.1	0.15	0.2
X_3 = BHC (% w/v)	0.01	0.055	0.1
Dependent variables	Constraints		
Y1 = Particle size (nm)	Minimize		
Y2 = Zetapotential (mV)	30 – 40		
Y3 = Encapsulation efficiency (%)	Maximize		

Table 2 Variables and observed responses in Box–Behnken design

Experiments	Factors combinations at different levels			Response variables		
	X_1 (%)	X_2 (%)	X_3 (%)	Y_1 (nm)	Y_2 (mV)	Y_3 (%)
BB1	0.2	0.1	0.055	216.5	25.4	71.52

BB2	0.6	0.1	0.055	278.4	19.8	67.08
BB3	0.2	0.2	0.055	423.4	45.2	63.54
BB4	0.6	0.2	0.055	472	38.1	61.13
BB5	0.2	0.15	0.01	298	21.9	76.48
BB6	0.6	0.15	0.01	323	15.1	72.31
BB7	0.2	0.15	0.1	267	19.8	79.18
BB8	0.6	0.15	0.1	345	13.7	75.34
BB9	0.4	0.1	0.01	240	16.8	68.79
BB10	0.4	0.2	0.01	468	30.4	60.58
BB11	0.4	0.1	0.1	272	15.2	65.32
BB12	0.4	0.2	0.1	488	28.8	66.54
BB13	0.4	0.15	0.055	302	25.4	85.69
BB14	0.4	0.15	0.055	308	26.2	82.56
BB15	0.4	0.15	0.055	311	24.8	79.48
BB16	0.4	0.15	0.055	308	25.8	77.76
BB17	0.4	0.15	0.055	305	26.8	81.45

Table 3: Summary of results of regression analysis for responses

Model	R^2	Adjusted R^2	%C.V	S.D	PRESS	Remarks
Response: Particle size (nm) (Y_1)						
Linear model	0.8812	0.8538	9.49	31.40	23988.13	-
Quadratic model	0.9930	0.9840	3.14	10.39	11412.13	Suggested
Special cubic model	0.9996	0.9983	1.03	3.42	ND[a]	-
Response: Zetapotential (mV) (Y_2)						
Linear model	0.5748	0.4766	24.10	5.94	952.45	-
Quadratic model	0.9841	0.9636	6.35	1.57	241.51	Suggested
Special cubic model	0.9979	0.9914	3.09	0.76	ND	-
Response: Encapsulation efficiency (%) (Y_3)						
Linear model	0.0923	-0.1171	11.40	8.28	1462.17	-
Quadratic model	0.9550	0.8972	3.46	2.51	177.34	Suggested
Special cubic model	0.9627	0.8507	4.17	3.03	ND	-

Table 4: Composition of optimum checkpoint formulations, the predicted and experimental values of response variables and percentage prediction error

Optimized formulation composition (X_1:X_2:X_3)	Response variable	Experimental value	Predicted value	Percentage prediction error
0.26 : 0.14 : 0.054	Y_1 (nm)	251.29	255.43	- 1.62
	Y_2 (mV)	25.73	26.43	- 2.65
	Y_3 (%)	80.91	81.21	- 0.37

Predicted error (%) = (experimental value − predicted value)/predicted value×100%

Table 5: Dissolution model study by fitting *in vitro* release study[a]

Model	Equation	R^2 Value
Zero order	mo - m = kt	0.8059
First order	ln m = kt	0.9893
Higuchi's model	mo - m = $kt^{1/2}$	0.9393
Korsmeyer–Peppas	log (mo - m) = log K + n log t	0.9531
Hixson–Crowell	$m_o^{1/3} - m^{1/3} = kt$	0.7849

[a] m_o is the initial drug amount (100%); m the amount of drug remaining at a specific time; k the rate constant; t is the time.

Table 6: Stability data

Time (days)	Entrapment efficiency (%)	Particle size (nm)	Zeta potential (mV)
0	79.84	257.43	22.98
30	78.76	249.69	24.82
90	80.91	251.29	25.73

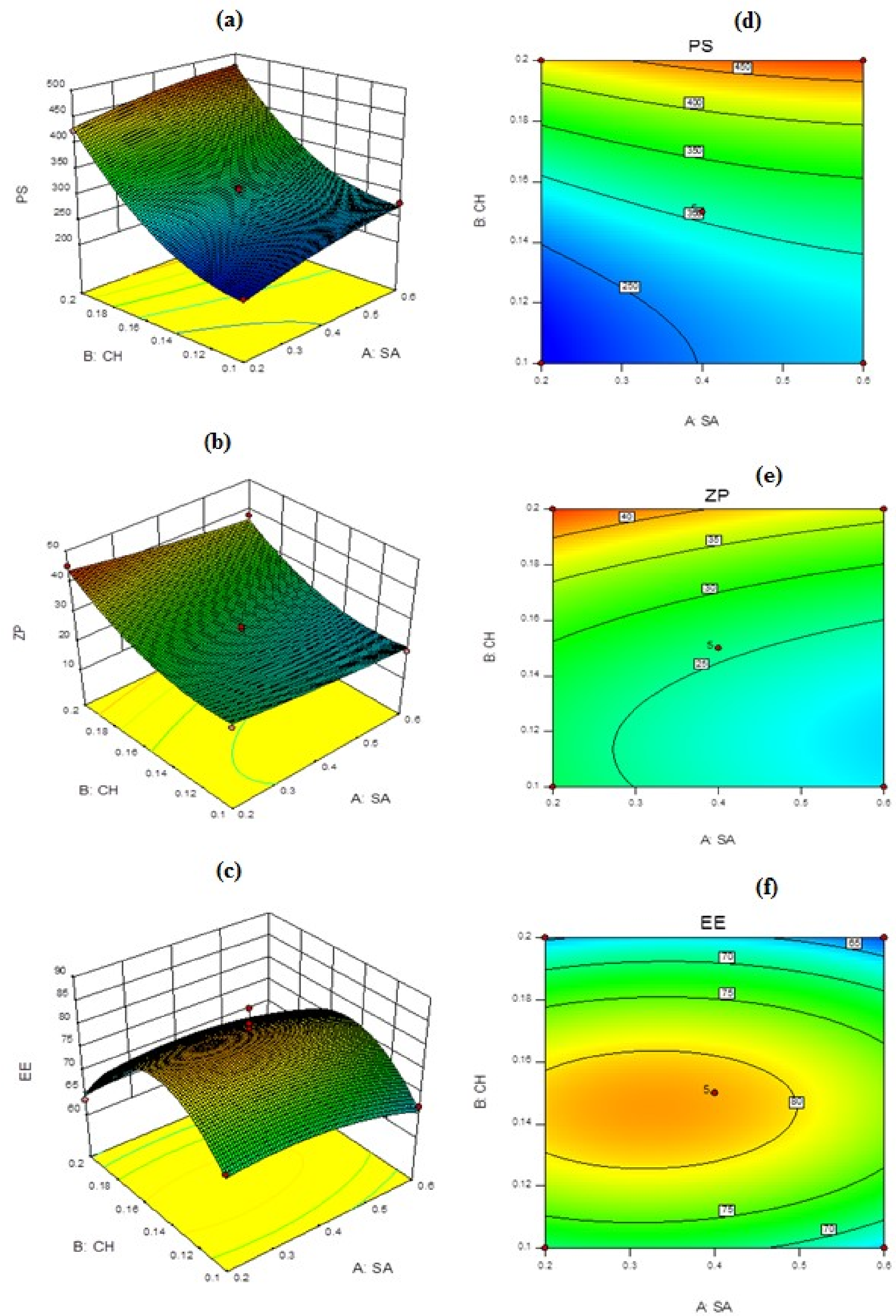

Figure 1: Effect of the contents of SA (X_1) and CH (X_2) on response using response surface plot (a–c) and its contour plot (d–f) at 0.055% (w/w) BHC level.

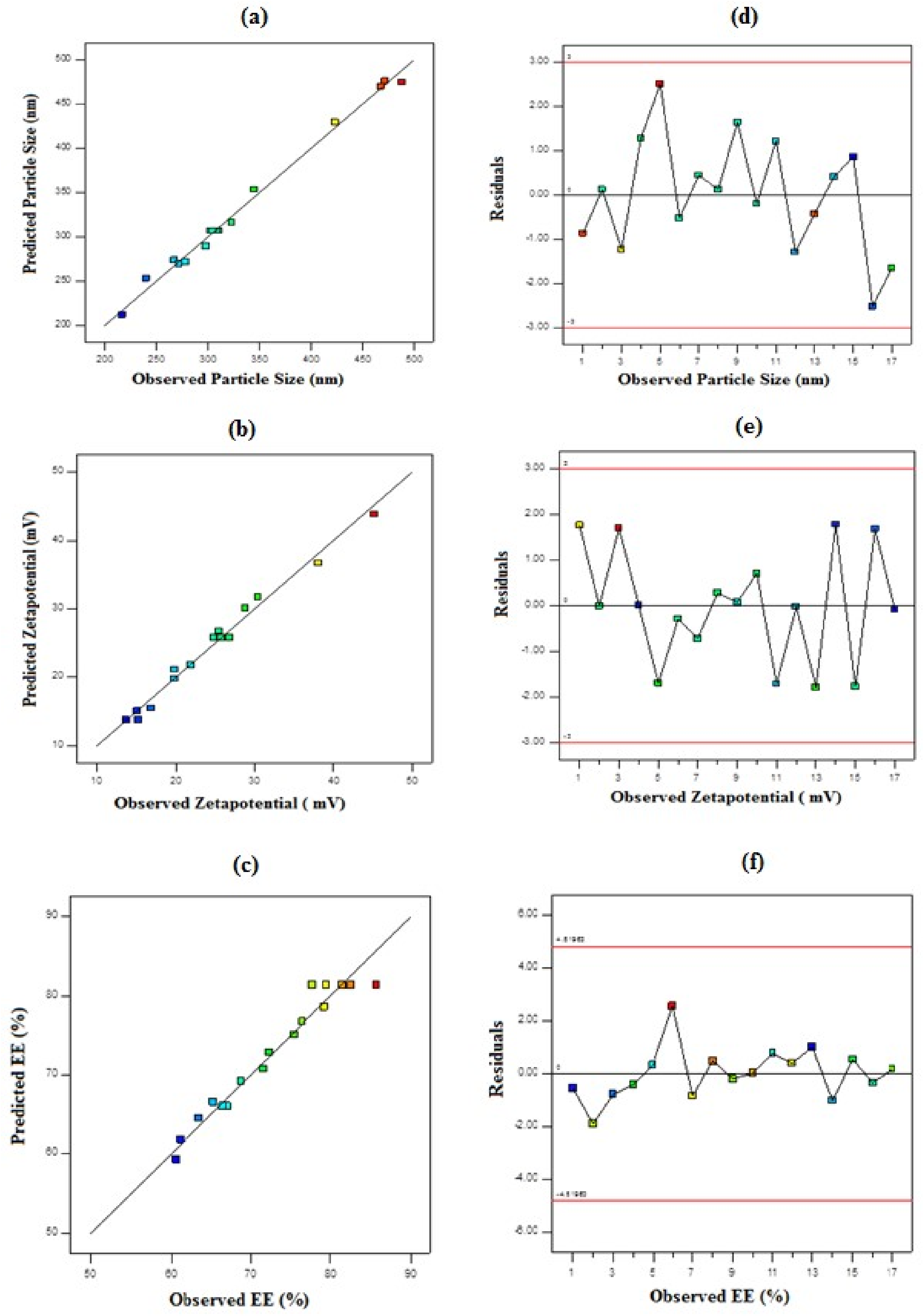

Figure 2: Linear correlation plots (a–c) between actual and predicted values and the corresponding residual plots (d–f) for various responses

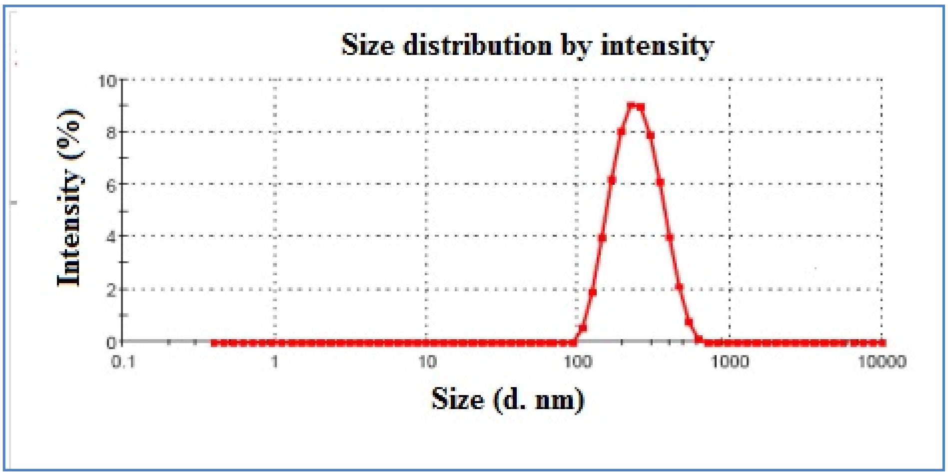

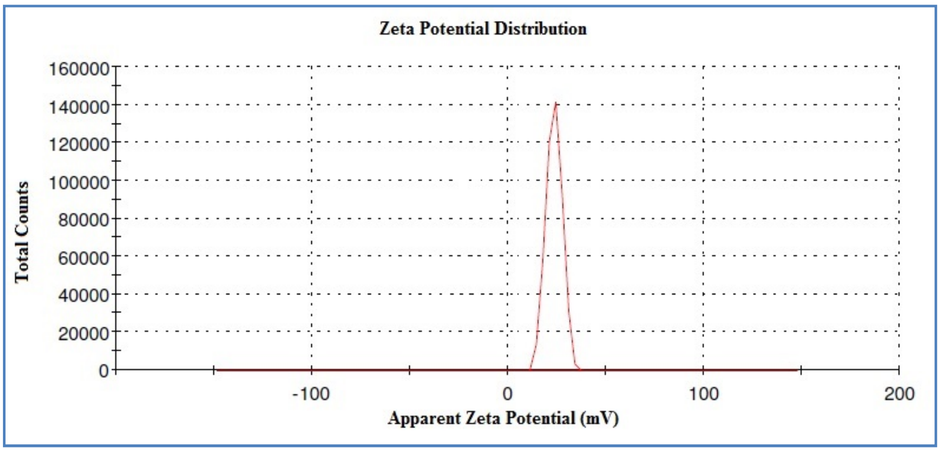

Figure 3: (a) Particle size and distribution of CH-SA nanoparticles (b) Zeta potential of CH-SA nanoparticle.

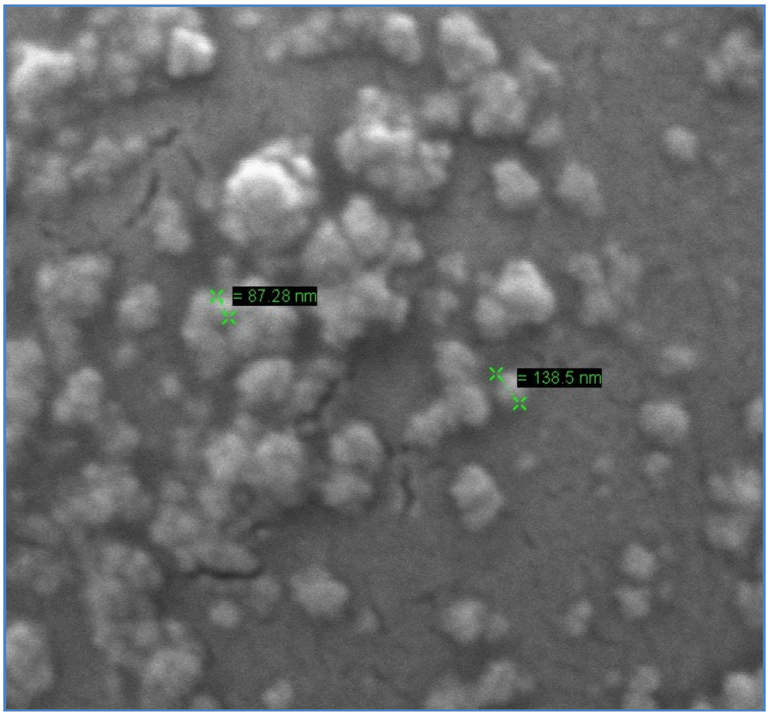

Figure 4: TEM image of BHC-loaded CH–SA nanoparticles.

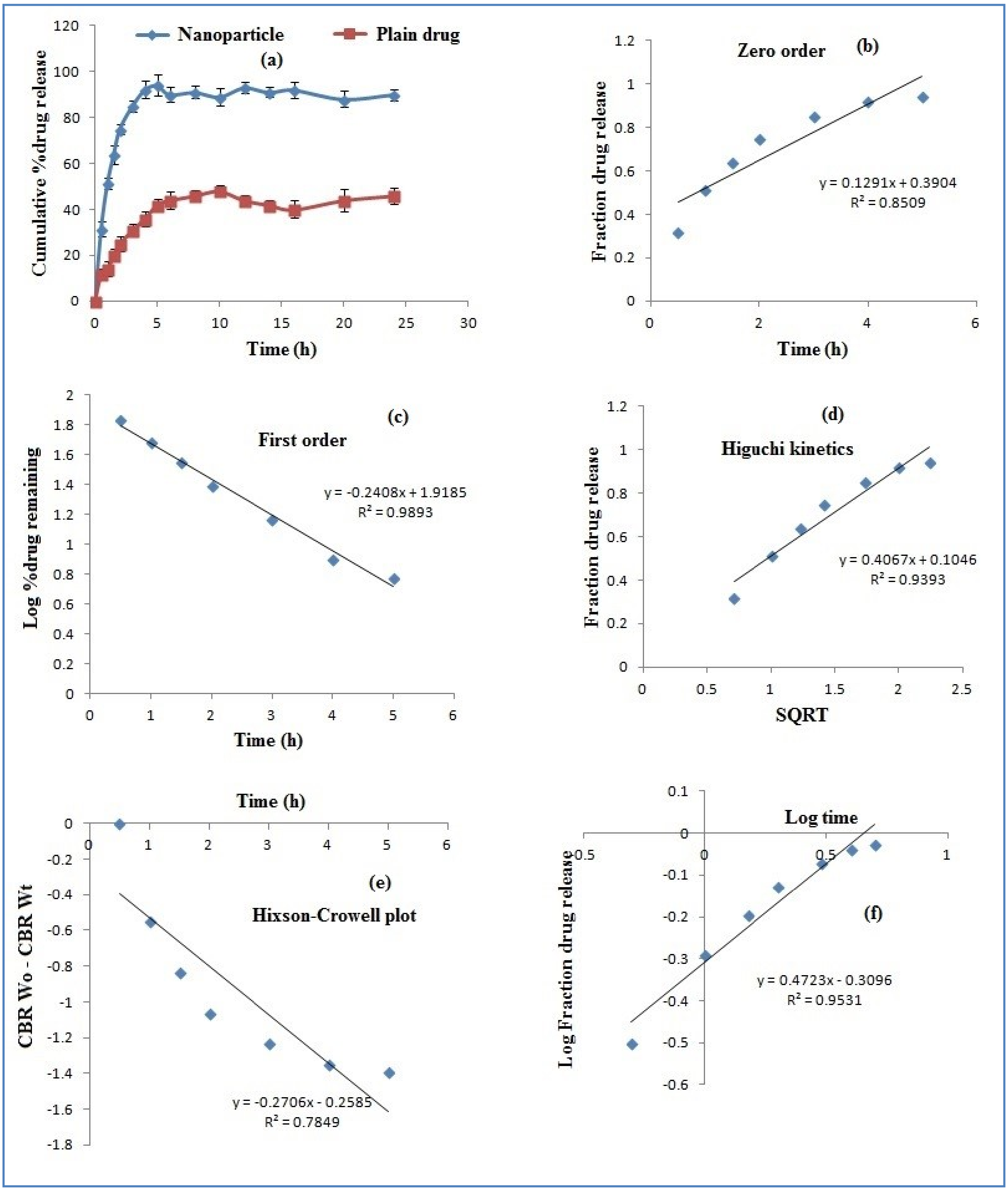

Figure 5: ***In vitro*** **release and release kinetics models for BHC-loaded CH–SA nanoparticles.**

4. CONCLUSION

This study was made to assess the usefulness of the CH-SA NPs system as a delivery agent for the anticancer drug BHC. In the present study, the potential of CS–SA NPs as drug carriers for oral delivery was investigated. The natural product berberine (BBR), a potential drug in the treatment of cancer, was successfully formulated in the form of CH–SA nanoreservoir system and the formulation was optimised by statistical screening design considering the concentration of CH, SA and BHC as independent variable.

The *in vitro* release profiles observed for these NPs were characterized by a burst initial release followed by a more gradual and sustained release phase. Our studies demonstrated that the new CH-SA NPs system of BHC is a promising strategy for improving solubility and in turn, therapeutic efficacy of BHC. The developed novel formulation has a potential application in treatment of cancer. CH-SA NPs system is commercially viable formulation of choice to give a new avenue of life to potential phytochemical berberine. In conclusion, this new nanosystem also offers an interesting potential for the delivery of hydrophobic compounds.

ACKNOWLEDGEMENTS

Authors have thankful for the financial support provided by Deanship of Scientific Research (DRS), Northern Border University under project grant number: PHM-2016-1-6-F-4609 to carry out this project.

Conflict of Interest:

Authors don't have any conflict of interest.

REFERENCES:

[1] Kim DW, Ahan SH, Kim TY, Enhancement of arsenic trioxide (As_2O_3)-mediated apoptosis using berberine in human neuroblastoma SH-SY5Y cells, J Korean Neurosurg Soc., 42(5), 2007, 392–399.

[2] Tsang CM, Lau EP, Di K, *et al.,* Berberine inhibits Rho GTPases and cell migration at low doses but induces G2 arrest and apoptosis at high doses in human cancer cells, Int J Mol Med., 24(1), 2009, 131–138.

[3] Singh T, Vaid M, Katiyar N, *et al.,* Berberine, an isoquinoline alkaloid, inhibits melanoma cancer cell migration by reducing the expressions of cyclooxygenase-2, prostaglandin E and prostaglandin E receptors, Carcinogenesis., 32(1), 2011, 86–92.

[4] Li-Weber M, Targeting apoptosis pathways in cancer by Chinese medicine, Cancer Lett.**,** 332(2), 2013, 304-312.

[5] Hsu WH, Hsieh YS, Kuo HC, *et al.,* Berberine induces apoptosis in SW620 human colonic carcinoma cells through generation of reactive oxygen species and activation of JNK/p38 MAPK and FasL, Arch Toxicol., 81(10), 2007, 719–728.

[6] Meeran SM, Katiyar S, Katiyar SK, Berberine-induced apoptosis in human prostate cancer cells is initiated by reactive oxygen species generation, Toxicol Appl Pharmacol., 229(1), 2008, 33–43.

[7] Katiyar SK, Meeran SM, Katiyar N, Akhtar S. p53 Cooperates berberine-induced growth inhibition and apoptosis of non-small cell human lung cancer cells in vitro and tumor xenograft growth in vivo, Mol Carcinog., 48(1), 2009, 24–37.

[8] Prabaharan M, Chitosan-based nanoparticles for tumor-targeted drug delivery, Int. J. Biol. Macromol., 72C, 2014, 1313–1322.

[9] Douglas KL, Tabrizian MJ, Effect of experimental parameters on the formation of alginate–chitosan nanoparticles and evaluation of their potential application as DNA carrier, J. Biomater. Sci. Polymer Edn., 16, 2005, 43–56.

[10] Yang Y, Wang S, Wang Y, *et al.,* Advances in self-assembled chitosan nanomaterials for drug delivery, Biotechnol. Adv., 32, 2014, 1301–1316.

[11] Agnihotri SA, Mallikarjuna NN, Aminabhavi TM, Recent advances on chitosan-based micro- and nanoparticles in drug delivery, J. Control. Rel., 100, 2004, 5–28.

[12] Janes KA, Fresneau MP, Marazuela A, *et al.,* Chitosan nanoparticles as delivery systems for doxorubicin, J.Control. Rel., 73, 2001, 255–267.

[13] Janes KA, Calvo P, Alonso MJ, Polysaccharide colloidal particles as delivery systems for macromolecules, Adv. Drug Deliv. Rev., 47, 2001, 83–97.

[14] Mi FL, Sung HW, Shyu SS, Drug release from chitosan–alginate complex beads reinforced by a naturally occurring crosslinking agent, Carbohydr. Polym., 48, 2002, 61–72.

[15] Mujtaba, A, Ali M, Kohli K, Formulation of extended release cefpodoxime proxetil chitosan-alginate beads using quality by design approach, Int. J. Biol. Macromol., 69, 2014, 420–429.

[16] Mujtaba, A, Ali M, Kohli K, Statistical optimization and characterization of pH-independent extended-release drug delivery of cefpodoxime proxetil using Box–Behnken design, Chem. Eng. Res. Des., 92, 2014, 156–165.

[17] Box GEP, Behnken DW, Some new three level designs for the study of quantitative variables, Technometrics, 2, 1960, 455–475.

[18] Pund S, Borade G, Rasve G, Improvement of anti-inflammatory and anti-angiogenic activity of berberine by novel rapid dissolving nanoemulsifying technique, Phytomedicine, 21, 2014, 307–314.

[19] Mujtaba A, Kohli K, In vitro/in vivo evaluation of HPMC/alginate based extended-release matrix tablets of cefpodoxime proxetil, Int. J. Biol. Macromol., 89, 2016, 434–441.

[20] Peppas NA, Analysis of Fickian and non-Fickian drug release from polymers, Pharm. Acta. Helv., 60, 1985, 110-111.

[21] Siepmann J, Peppas NA, Modeling of drug release from delivery systems based on hydroxypropyl methylcellulose (HPMC), Adv. Drug Deliv. Rev., 48, 2001, 139-157.

[22] Kim MS, Kim JS, You YH, et al., Development and optimization of a novel oral controlled delivery system for tamsulosin hydrochloride using response surface methodology. Int. J. Pharm., 341, 2007, 97–104.

[23] Douglas KL, Tabrizian MJ, Effect of experimental parameters on the formation of alginate–chitosan nanoparticles and evaluation of their potential application as DNA carrier, J. Biomater. Sci. Polymer Edn., 16, 2005, 43–56.

[24] Segurola J, Allen NS, Edge M, *et al.,* Design of eutectic photoinitiator blends for UV/visible curable acrylated printing inks and coatings, Prog. Org. Coat., 37, 1999, 23-37.

[25] Motwani SK, Chopra S, Talegaonkar S, *et al.,* Chitosan-sodium alginate nanoparticles as submicroscopic reservoirs for ocular delivery: formulation, optimisation and *in vitro* characterisation, Eur J Pharm Biopharm., 68(3), 2008, 513-525.

[26] Kotze AF, Thanou MM, Luebetaen HL, *et al*., Enhancement of paracellular drug transport with highly quaternized N-trimethyl chitosan chloride in neutral environments: *In vitro* evaluation in intestinal epithelial cells (Caco-2), J. Pharm. Sci., 88, 1999, 253-257.

[27] Yan XL, Khor E, Lim LY, Chitosan-alginate films prepared with chitosans of different molecular weights, J. Biomed. Mater. Res., 58, 2001, 358-365.

[28] Simsek-Ege FA, Bond GM, Stringer J, Polyelectrolyte complex formation between alginate and chitosan as a function of pH, J. Appl. Polym. Sci., 88, 2003, 346–351.

[29] Chopra S, Patil GV, Motwani SK, Release modulating hydrophilic matrix systems of losartan potassium: Optimisation of formulation using statistical experimental design, Eur. J. Pharm. Biopharm., 66, 2007, 73–82.